Quality factor control in a lasing microcavity model

Ioana Triandaf and Ira B. Schwartz
Special Project in Nonlinear Science, U.S. Naval Research Laboratory, Code 6700.3, Plasma Physics Division, Washington, D.C. 20375-5000

(Received 25 January 1999; revised manuscript received 5 December 1999)

We consider a dynamics model of lasing microcavities, a class of optical resonators (1–10 μm in diameter) used in microlasers and for optical coupling of optical fibers. Inside such a cavity light circulates around the perimeter and is trapped by internal reflection. This is known as ''whispering gallery'' or high-Q modes. The cavity is a deformable cylindrical (or spherical) dielectric and at certain deformations light can escape by refraction. The quality of the resonator or Q factor, is defined as $Q=\omega\tau$, where τ is the escape time and ω is the frequency of light. We show that by appropriately deforming the cavity, the Q factor can be controlled by prolonging or shortening the average length of time spent by light trajectories inside the cavity.

PACS number(s): 05.45.Gg, 05.45.Mt

I. INTRODUCTION

Laser resonators are components in lasers used to generate light with desired frequencies. Typically, the desired quality of light is achieved by feeding back the light into the laser using mirror arrangements. The same feedback effect using mirrors can be achieved in a number of semiconductors of spherical or cylindrical shape, by creating an internal reflection of the electromagnetic wave just inside the surface of the dielectric cavity. A large difference between the index of refraction of the semiconductor and that of air ensures a long residence time of the light inside the cavity before it escapes due to refraction. This ensures the exceptionally high quality of the emitted light, for which these resonators are known [1,2].

These cavities are dielectric bodies that have spherical or cylindrical symmetry and the waves circulating inside these microcavities are called ''morphology-dependent resonances.'' Another name used for these modes is ''whispering gallery'' modes, the name first used by Lord Raleigh when explaining the efficient propagation of sound (even of whispers) along the walls of St. Paul's cathedral. The quality of such a resonator Q is defined by $Q=\omega\tau$, where ω is the mode frequency and τ its lifetime inside the cavity.

The study of optical microresonators is under way in a wide variety of condensed matter systems, such as semiconductor microlasers [1]. Due to the exceptionally high Q factor, these devices have the potential for the reduction of the lasing threshold required for large scale photonic integration [3,4]. Ideally only one mode or just a few modes of the optical field are isolated in such a cavity. High-Q modes have been studied in optical fibers [5], liquid droplets [6], and glass spheres [7] for the purpose of understanding nonlinear optical effects and to investigate the interaction of atoms with single cavity modes [8]. In Fig. 1 we reproduce from Ref. [9] the images of real lasing microdisks used in real experiments, which were obtained with a scanning electron microscope. These devices are under 5 μm in diameter. In [9] it is shown that these devices can be reliably fabricated and have the potential for low-power operation, a requirement for efficient functioning of these devices when coupled in microphotonic circuits and arrays.

In this paper we address the issue of controlling the Q factor of such cavities by controlling the residence time of light inside the cavity. Spontaneous emission due to deformation is a major source of energy loss. Improved performance of the microresonator can be obtained by maintaining light inside the cavity longer in order to increase the Q factor. As pointed out in Ref. [10] it is desirable to build deformable cavities and use the deformation as a Q-factor switch for dumping out stored light at will, the potential application being in the coupling of optical fibers [11].

For small deformations or when the microresonator is small compared to the wavelength of the circulating light, the process is modeled by the wave equation [12]. For high deformations and when the cavity is large compare to the wavelength, ray-optics models have been proposed [10,13] which we use in this paper to illustrate our control methods.

The ray-optics model introduced in [10] is a Hamiltonian map, the iterates of which represent the consecutive bounces of a light ray against the cavity. This map obeys the Kol'mogorov-Arnol'd-Moser (KAM) theorem of classical mechanics: as the deformation grows the dynamics becomes increasingly chaotic following a KAM type of scenario [14]. The ray dynamics inside the cavity is equivalent to the nonlinear dynamics of a point mass undergoing reflections from the walls of a two-dimensional ''billiard,'' a problem that has been extensively studied in mechanics [15]. Different deformations of the boundary generate very different types of orbits. In the mechanics setting the focus is on quantum mechanics and ergodic theory issues [16]. The trajectories inside the cavity become chaotic at high deformations which correspond to large angles of incidence of the rays at the boundary. For small values of the angle of incidence the rays get reflected back into the cavity, while for angles above a certain critical value escape occurs by refraction according to Snell's law.

In real devices the deformation of the cavity occurs due to inertial forces, trapping electric fields or laser-induced electrostriction [10], and spoiling of the Q factor is observed. In an ideally lossless cavity the Q factor can be also spoiled by evanescent leakage (tunneling) [10]. Using a ray-optics point of view [17], escape occurs when the angle of incidence of a

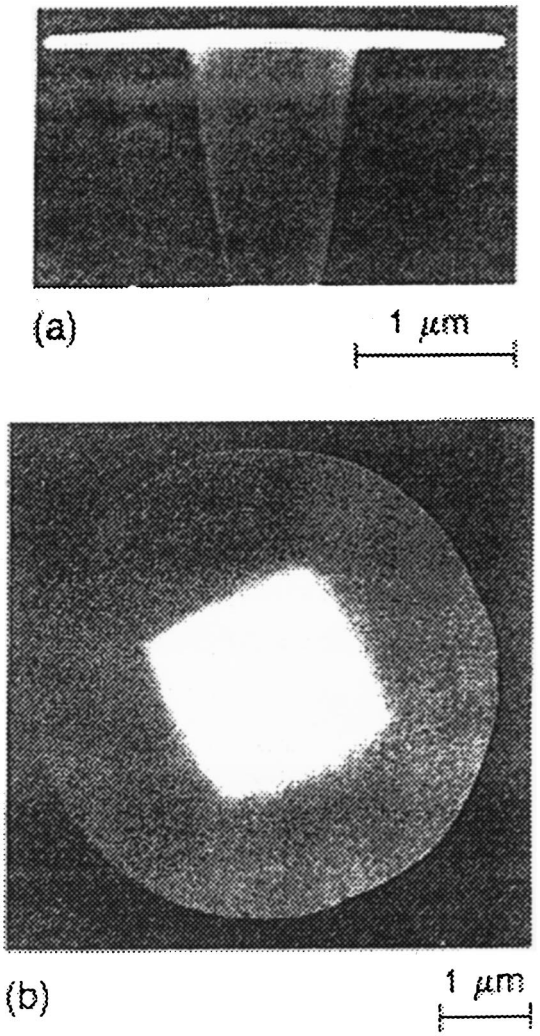

FIG. 1. Images of microdisks obtained with a scanning electron microscope: (a) side view of a disk with a 3-μm diameter, (b) top view of a disk 5 μm in diameter.

ray at the boundary reaches a critical value given by Snell's law.

Related work on control can be found in [18], where the author shows how chaos in microcavities can be eliminated in favor of regular behavior by coupling the field inside the cavity with another pump field. Methods for the control of Hamiltonian systems such as the one in [19] could not be used for our system, since they require close monitoring of the dynamics inside the device, which in our case takes place with the speed of light. The method presented in [20] could not be used for our system, since that method requires modifying the equations of state of the system. In our case these equations are implicit, being obtained from geometric considerations.

The paper is organized as follows: we present the ray model and discuss its dynamics in Sec. II. In Sec. III we show how to shorten or lengthen the residence time of light inside the cavity by pulsing the deformation parameter: regular, small amplitude pulses can be used to shorten the residence time. To lengthen it, we show that a few large amplitude pulses, applied as early as possible, can be used. We also show that designing the cavity out of layers of material

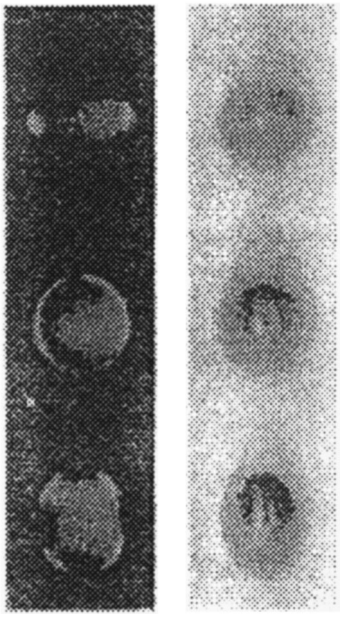

FIG. 2. Shadow graphs and simultaneous total-intensity images of three lasing droplets falling in air taken at different phases of oscillation.

with a different refraction index leads to delaying emission.

II. THE RAY MODEL AND ITS DYNAMICS

To motivate the control results and get a better intuition of the phenomenon we address, we refer to an experiment done with lasing liquid droplets [2]. In Fig. 2, reproduced from [2], we show three ethanol droplets falling in air. These droplets contain a lasing dye and emit light [21]. In one column we see shadow graph images of the falling droplet. Next to it we see the corresponding total-intensity images of the emission patterns. The droplets take different shapes as they are falling and the emission pattern varies according to the shape of the droplet. The deformation thus determines the dynamics inside the cavity.

Although the microcavities can be spheres, disks, or cylinders, in what follows we will describe a model for a two-dimensional lasing microcavity (a disk) [10]. The shape of the cavity is described by a conformal transformation of the unit disk ([3]) which was first introduced in [16],

$$w(z)=\frac{z+bz^2+cz^3}{(1+2b^2+3c^2)^{1/2}}, \tag{1}$$

where b and c are real parameters, and $z=e^{i\phi}$, $0\leqslant\phi<2\pi$.

The dynamics is thus four dimensional in position-momentum space. To represent it one reduces it to a lower-dimensional map which defines the angle of incidence α as a function of the arc length ϕ (a two-dimensional cut through a four-dimensional phase space). This map represents a Poincaré section of the original phase space. In Fig. 3 we show the coordinates used for the Poincaré section. We emphasise that the angle of incidence in this paper is measured from the tangent to the cavity towards the ray, which leads to figures of the dynamics reversed compared to the corresponding ones in [10]. The figures of the dynamics in what follows will be represented in terms of the angle of incidence at the

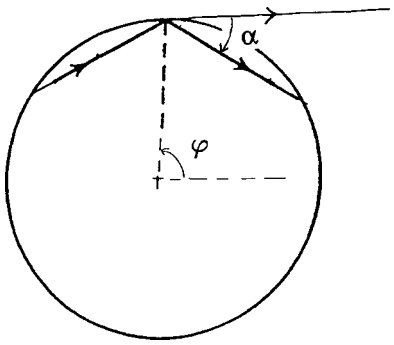

FIG. 3. Definition of the coordinates for the Poincaré section used to analyze the ray dynamics inside a disk.

boundary versus the arc length. To represent a trajectory one has to determine the successive values of the arc length and of the angle of incidence at each bounce. Having determined $(\phi_n, \sin(\alpha_n))$ the next values $(\phi_{n+1}, \sin(\alpha_{n+1}))$ are determined from geometric considerations, without an explicit formula. In [21] it is shown that the correspondence which associates the coordinates at the nth bounce $(\phi_n, \sin(\alpha_n))$ to the coordinates at the $(n+1)$th bounce $(\phi_{n+1}, \sin(\alpha_{n+1}))$ defines a nonlinear map. This map is defined implicitly from geometric considerations [15] and requires using a Newton method for determining the arc length ϕ_{N+1} from the previous iteration. The angle of incidence is determined easily as follows:

$$\alpha_{n+1} = \psi_{n+1} - \psi_n - \alpha_n, \tag{2}$$

where ψ_n stands for the direction of the forward tangent at the nth iterate. The practical construction of this map can be found in detail in [15].

We study the dynamics of the phase space when several light rays are sent into the cavity at uniformly distributed angles of incidence, as the deformation parameter b is varied, while we hold $c=0$ fixed. Figures 4, 5, and 6 show the phase space at different deformations. For the undeformed cavity $(b=0)$ the trajectories are periodic: appearing as a series of points in the Poincaré surface of section (not shown) or tori (quasiperiodic orbits) appearing as continuous dotted lines, as shown in Fig. 4(a). A real quasiperiodic trajectory, in this regime, is shown inside the cavity [Fig. 4(b)], next to the Poincaré surface of section for several trajectories [Fig. 4(a)].

To have escape, the angle of incidence has to satisfy Snell's law,

$$\sin(\alpha) \geq \frac{1}{n}, \tag{3}$$

where n is the ratio of the refraction index of air over the refraction index of the dielectric. In what follows we will call the critical angle the angle of incidence for which Eq. (3) holds with an equality sign.

As the deformation increases, say to $b=0.11$ some tori get deformed whereas others break down giving rise to new motions on a tori as well as to an equal number of elliptic and hyperbolic periodic orbits. This result follows from the Poincaré-Birkhoff theorem [14]. Around the new elliptic orbits new tori form, nested around that orbit. The configuration of tori surrounding a periodic elliptic orbit is called an island chain. In Fig. 5(a) we see the island chains in the Poincaré surface of section phase space, along with uninterrupted quasiperiodic trajectories which persisted under the deformation. In Fig. 5(b) we show a trajectory, inside the disk, corresponding to an island chain with four islands.

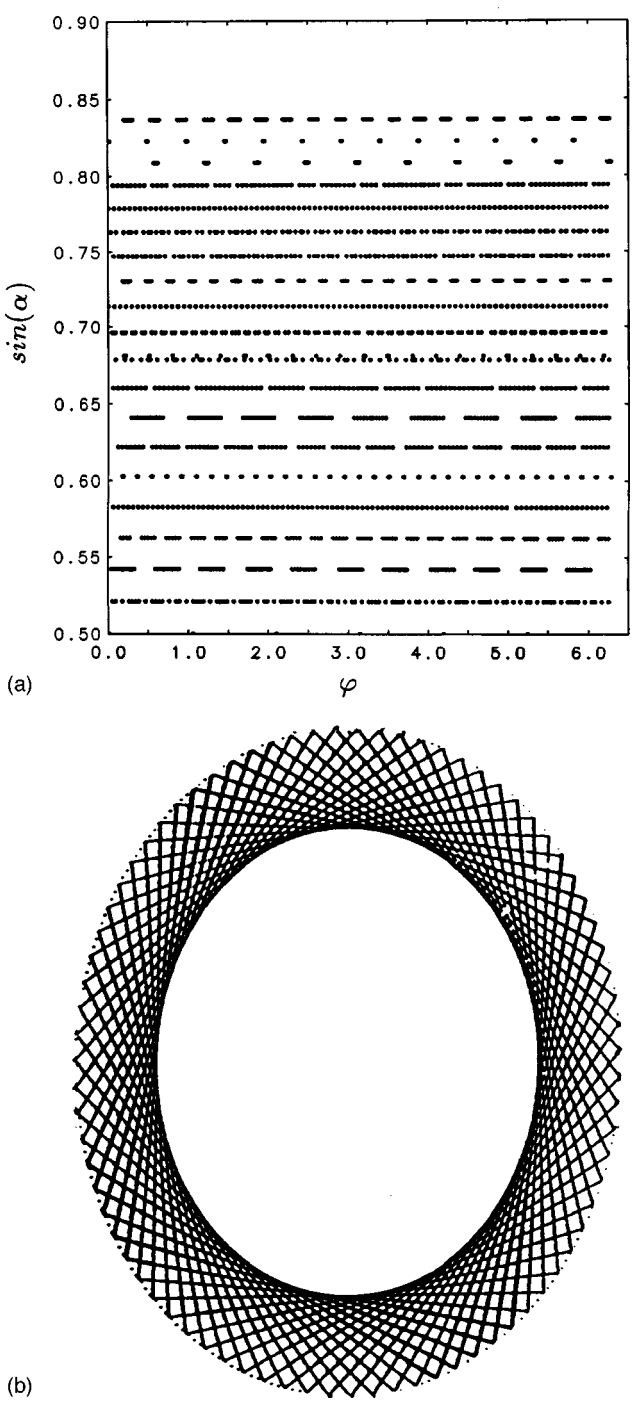

FIG. 4. (a) The phase space for the Poincaré section when no deformation is present $(b=0)$. (b) Typical quasiperiodic trajectory at $b=0$ inside the cavity.

As the deformation parameter is further increased the region occupied by tori that break increases giving rise to more and more islands chains and more and more hyperbolic orbits. The island chains themselves break down in the same way the original tori broke down giving rise to more elliptic

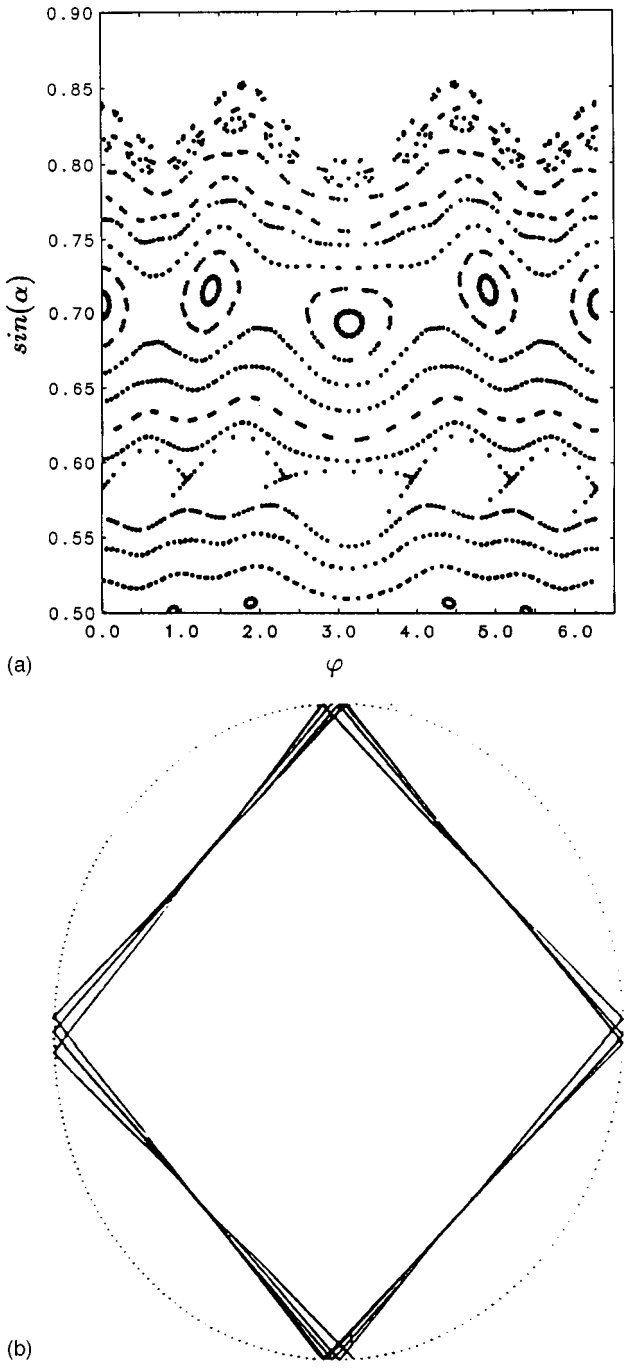

FIG. 5. (a) The phase space for the Poincaré section at $b = 0.11$ showing island chains and deformed quasiperiodic trajectories. (b) Trajectory at $b = 0.11$, which corresponds in phase space to an island chain with four islands.

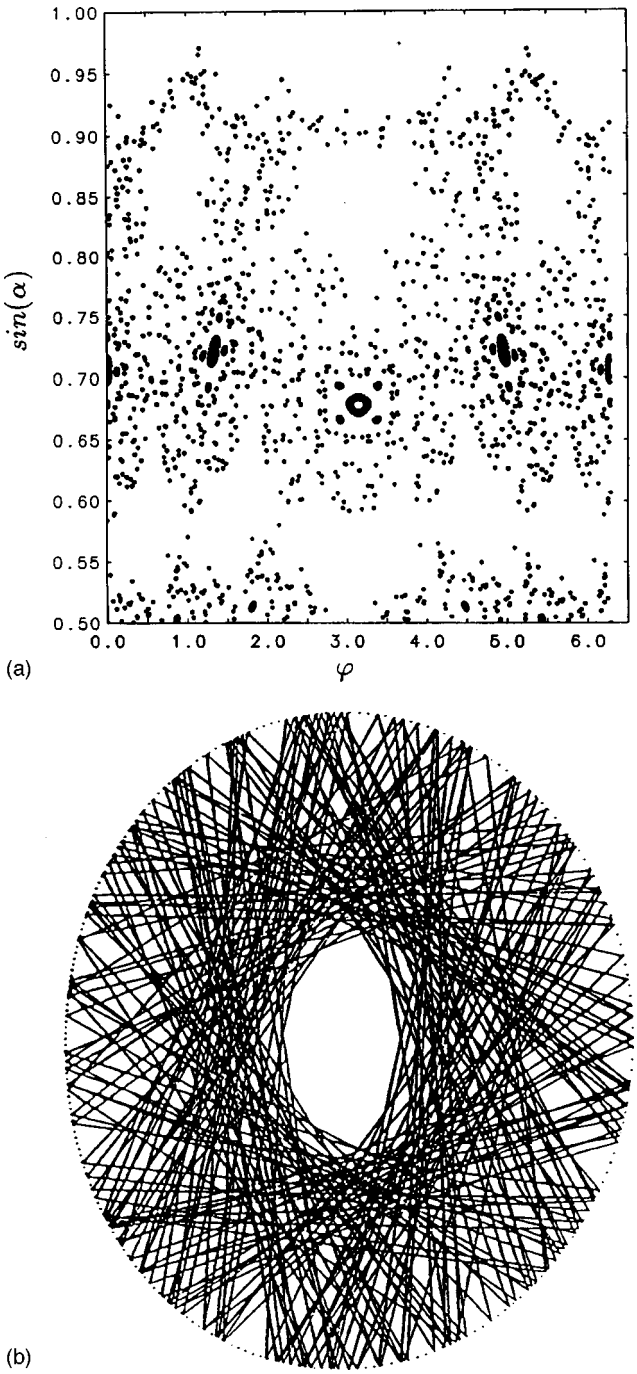

FIG. 6. (a) The phase space at a high deformation $b = 0.15$, showing chaos in the upper region, island chains and quasiperiodic trajectories. (b) Chaotic trajectory inside the cavity.

and hyperbolic orbits. The hyperbolic orbits that appear are leading to the formation of chaos. The stable and unstable orbits emanating from a hyperbolic orbit form heteroclinic intersections [14]. One such heteroclinic intersection implies an infinite number of them [14], which implies the presence of horseshoe-type dynamics and hence chaos. As b increases larger regions of phase space become occupied by chaos. In Fig. 6(a) we see the phase space at $b = 0.15$. We also show a typical chaotic orbit [Fig. 6(b)] inside the cavity.

Without chaos the angle of incidence of rays inside the cavity remains bounded. When chaos starts to appear some of the tori break down and a light ray can migrate in between island chains towards regions of phase space corresponding to a higher angle of incidence, eventually reaching the critical value which satisfies Snell's law and escape occurs. The trajectories that appear to be chaotic in this model are indeed chaotic since we have found that the Lyapunov exponents for these trajectories are positive, typical maximum values being around 0.13 when calculated over 1000 iterates of the map.

III. CONTROL OF THE Q FACTOR

One defines the quality of the resonator, or Q factor [10], as $Q = \omega\tau$, where τ is the escape time and ω is the frequency

of light. When injecting light inside the dielectric, within a given angle of incidence,

$$\alpha_1 < \sin(\alpha) < \alpha_2,$$

if the cavity is deformed, so that sufficient chaos is present, escape can occur. One would like to be able to control the mean residence time of these rays inside the cavity. To calculate the mean residence time we observe the dynamics over a fixed number of iterations (bounces) of the rays, say 1000, then add up the escape time of each ray and divide by the total number of trajectories. The rays which do not escape during the observation are considered to have escape time the length of the observation, that is 1000.

In this section we will show first how we can dump out stored light at will by pulsing regularly the deformation parameter. Second, we will show how we can prolong the mean escape time also using the deformation parameter. In the last numerical example we will show that if the cavity is made out of layers of different refraction indices, escape can be prevented very effectively.

The control we propose is open loop control, and acts by adjusting the deformation parameter. The cavity has been already deformed to a value at which chaos is present and escape occurs. We want to influence the escape time, delay it or shorten it, by giving extra deformations to the cavity at carefully chosen intervals of time. In practice [11] this could be achieved, for example, by piezoelectric devices, acting on the cavity at prescribed intervals of time.

The first approach we consider for control is to deform the cavity slightly, at regular intervals of time,

$$b = b_0 + \delta b, \tag{4}$$

where b_0 corresponds to the deformation already present and δb is a brief pulse given at regular time intervals. To quantify the amount of deformation, we define the eccentricity to be

$$e = (r_{\max}^2 - r_{\min}^2)/r_{\max}^{1/2}, \tag{5}$$

where $r_{\max}$ and $r_{\min}$ are, respectively, the maximum and minimum radius of the cavity, measured from the center of mass. With this definition, at $b = 0.15$ the eccentricity equals 0.47 and the extra amount of deformation we allow represents approximately 8% of the deformation already present. We found that by regularly pulsing the deformation parameter b escape is provoked faster, i.e., the escape time is shortened by at least one-third. We considered 30 rays launched into the cavity over a range of angles, α, so that $0.7 < \sin\alpha < 0.8$, at $b = 0.15$ and observed the trajectories over 1000 iterations, as extra deformations are given with various amplitudes and frequencies. We tried several amplitudes of the pulse and several frequencies and the results are shown in Fig. 7. This is a color map of the escape time: the coordinates on this map are the frequency of the pulse (dimensionless) versus the amplitude of the pulse. The frequency is measured in the number of map iterations in between control pulses. The colors on the map stand for different escape times, from short escape times corresponding to light colors to long escape times corresponding to dark colors. In this figure, we increased the amplitude δb by 0.01 and the frequency by 5 before each control experiment. 5 means number of iterates of the map, i.e., the number of bounces of a light ray against the cavity. Each point on the map corresponds to fixed values of the amplitude and of the frequency. We ran this numerical experiment on a supercomputer due to the large number of times we need to solve a nonlinear equation by the Newton method. Next we sample cross sections of this color map, horizontally and vertically; that is, we fix the frequency and let the amplitude vary and then fix the amplitude and vary the frequency. In Fig. 8 we took slices of the color map at frequencies equal to 30 iterates and 74 iterates. What we see from these plots is that at fixed frequency the larger the amplitude of the pulse the faster the escape time. This trend is present at low as well as high frequencies. In these plots the amplitude was varied by $\delta_{\text{amp}} = 0.01$. If we refine this step we would see the same trend but a more irregular curve. So the escape time can be predicted within a good accuracy, the error in prediction being at most ten iterations. In Fig. 9 we took a horizontal cut of the map in Fig. 7. What we notice is that at low amplitudes, that is small pulses, say $\delta_b = 0.03$ the escape time oscillates around the same value. The escape time is well below the escape time without control (which is 750 iterations), but stays roughly the same. If we consider larger pulses, say $\delta_b = 0.045$, we notice that the escape time decreases rapidly as we increase

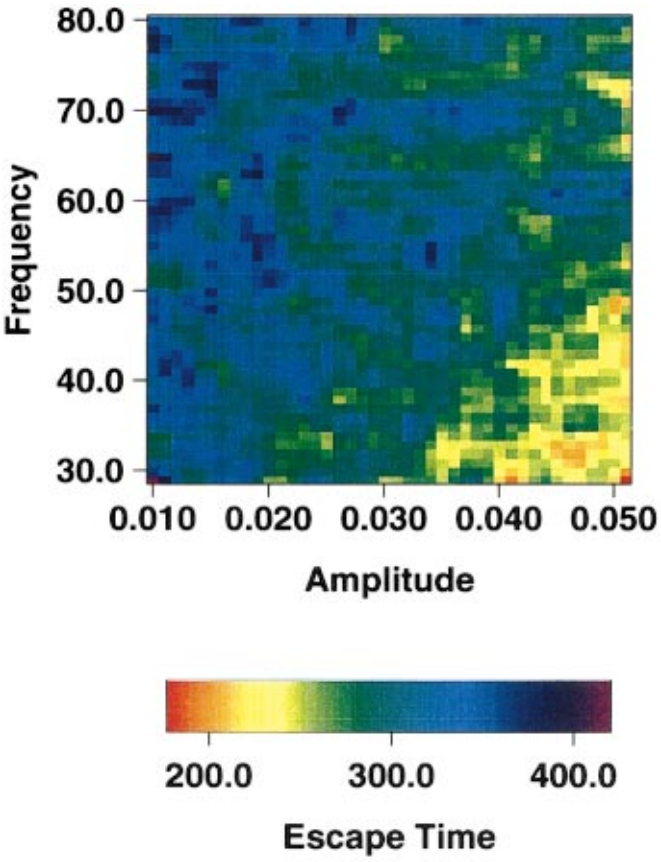

FIG. 7. (Color) Color map of the mean escape times when 20 rays were injected into the cavity and observed for 1000 iterations. These rays initiate with an angle of incidence such that $0.7 < \sin(\alpha) < 0.8$. The escape ratio of indices was set at 0.9. One point on this map represents the escape time for a fixed amplitude and frequency of the deformation pulse. The darker the color the longer the escape time.

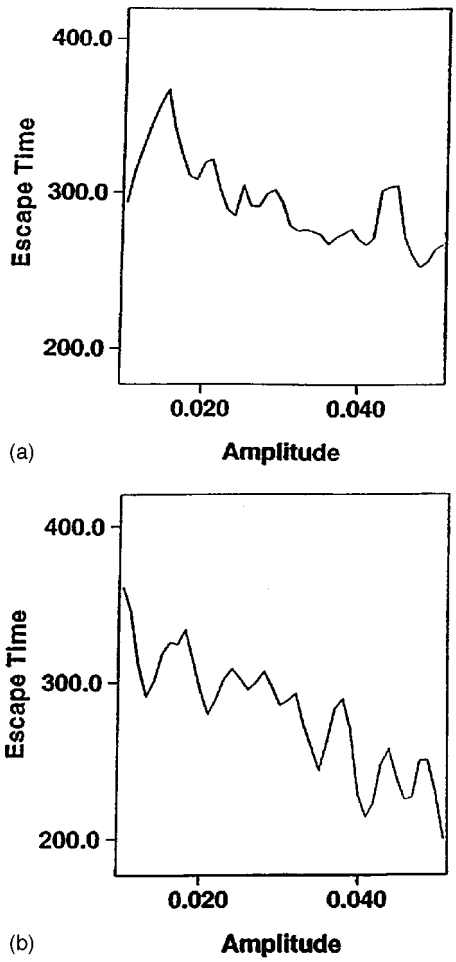

FIG. 8. (a) Mean escape times when the frequency of the pulse is 74 iterations and the amplitude is varied in steps of $\delta_{\text{amp}}=0.01$. (b) Mean escape times when the frequency of the pulse is 30 iterations.

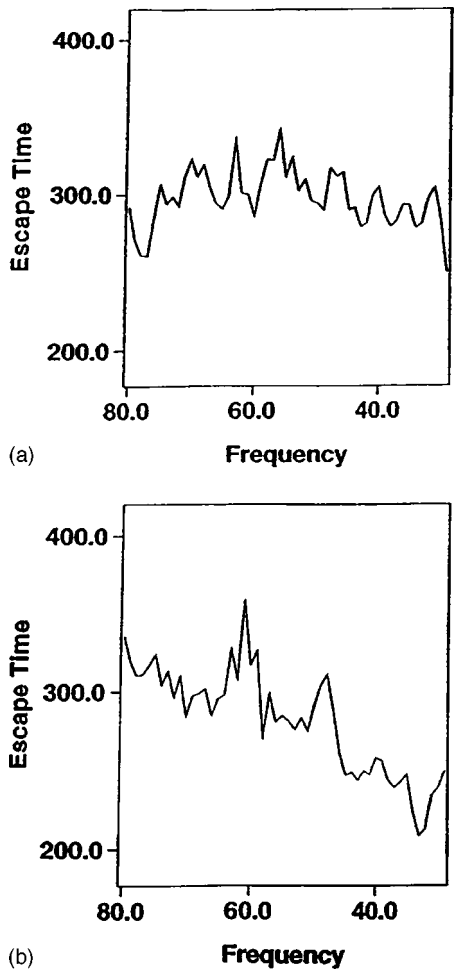

FIG. 9. (a) Mean escape times when the amplitude of the pulse is 0.03; the frequency was varied with a step $\delta\nu=1$. (b) Mean escape times when the amplitude of the pulse is 0.045.

the frequency of the pulse. As before the average escape time can be predicted from these plots within an error of at most 10 iterations.

In the above numerical experiments the starting values of the incidence angle $0.7<\sin\alpha<0.8$ were purposefully chosen close to the escape value $\alpha=0.9$ in order to minimize the computer time. It also demonstrates the effectiveness of the control. In addition, the number of maps was chosen large enough to illustrate the trends in control. Even so, the runs take several minutes on a supercomputer due to the large number of Newton equations that have to be solved at each iterate since the map is given implicitly. In a real device, the method of control can be argued to be realistic only at small deformations when the Q factor is large. With a large enough Q, say $Q\gtrsim 10^6$, the above method of control can be implemented electro-optically which requires a control time of the order of nanoseconds [11]. An actual mechanical deformation would take much longer by several orders of magnitude. Instead, the effect of a mechanical deformation can be replaced by locally lowering the refraction index electro-optically. An instantaneous local change in the refraction index would temporarily modify (lower) the escape value which is equivalent to an instantaneous change in the deformation parameter.

We did not find any values of the amplitude and of the frequency of the pulse at which the escape time gets delayed. So this type of control cannot be used to prolong trajectories. For control we can interfer only with external pulses, which are difficult to connect with the dynamics inside the cavity, given the speed of the process—the speed of light. So it was more difficult to find an open loop control method which would delay the escape time. The idea was that it would be good to recreate, by some external deformations, some of the quasiperiodic trajectories that are present at $b=0$, which appear in phase space as uninterrupted lines. These type of trajectories do not allow escape of trajectories circulating at lower angles of incidence in phase space. We have found that this can be realized by giving a large amplitude pulse or just a few large amplitude pulses close to the beginning of the numerical experiment. These pulses should be applied so that b decreases, i.e., the deformation is temporarily reduced. The size of these pulses is of the same order as the deformation. These pulses are more efficient, in terms of getting longer trajectories, the earlier they are applied in the numerical experiment. In Figs. 10 and 11 we illustrate this procedure. In Fig. 10 we see the phase space without any control when the mean escape time is 1759 iterations and the phase space shows angles of incidence between 0.7 and 0.9. We assume in this experiment that the escape angle is at 0.9. In

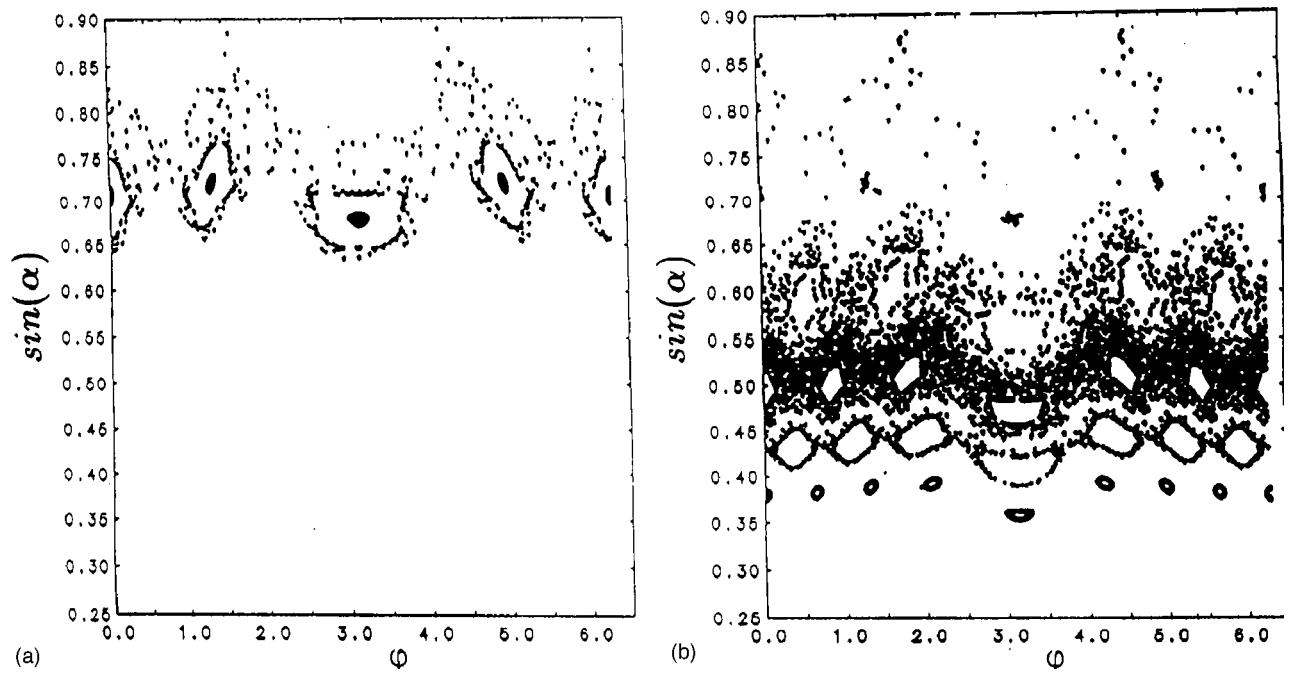

FIG. 10. (a) 20 trajectories at $b=0.15$ with a mean escape time of 1759 iterations when observed over 3000 iterations. (b) The same trajectories when two pulses of amplitude $\delta b=0.05$ were given at 60 iterations and at 90 iterations. This time the mean escape time was increased to 2280 iterations, that is by 30%.

Fig. 10(b) we show the phase space when we gave two large pulses, one after 60 iterations and one after 90 iterations. The trajectories were pushed towards much lower angles of incidence so it will take much longer for trajectories to migrate towards the escape angle. We notice that instead of two layers of islands we have five layers of islands present, which limits the space through which trajectories can escape towards higher angles of incidence. The mean escape time was prolonged by 29.6%. In a second numerical experiment shown in Fig. 11 we gave a single large pulse after 90 iterations using the same initial phase space as before. The new phase space looks very different than in the example before [Fig. 10(b)] and the mean escape time was prolonged by 8.8%. As before we see that more island chains appeared and the trajectories spread over a larger range of angles of incidence. In adition some unbroken tori were created as expected initially in this procedure. These two examples show that the escape time and the phase space obtained, will be quite different according to how these pulses are given. Still, once the number and the timing of the pulses is fixed, the

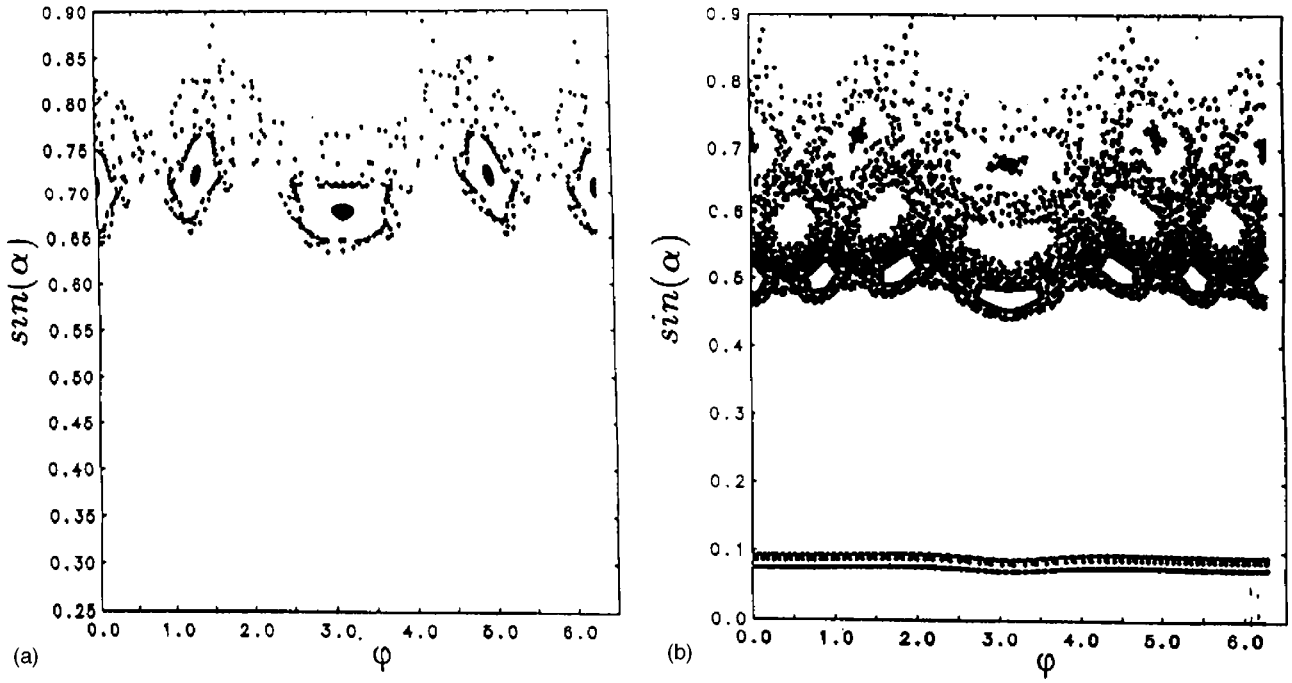

FIG. 11. The same number of trajectories as in Fig. 10 when a pulse of amplitude $\delta b=0.1$ was given after 90 iterations.

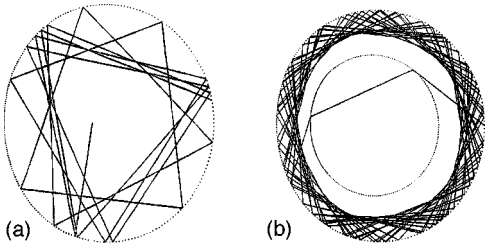

FIG. 12. (a) A chaotic trajectory escaping in 25 iterations. (b) The trajectory with the same initial conditions as in (a) inside a disk made of two layers, the refraction index of the outer layer is smaller then the index of the inner layer.

process is robust to errors in these parameters. Heuristically, what this procedure does is to re-establish for a very brief amount of time the undeformed shape. We notice that this is enough to make some of the features of the dynamics at lower deformations reappear, namely islands chains and unbroken tori which form barriers for escaping trajectories.

The above values of the escape time were chosen only for the purpose of demonstration. In a real microdisk the escape can happen within picoseconds, and for the above method to be realistic, control has to be applied (electro-optically) at the same time when the light is injected in the cavity. Since the control is designed to be open loop, it does not require feedback knowledge, which increases its probability of success.

An alternate way to prolong the escape time is to design the cavity out of layers with a different refraction index. In Fig. 12(a) we show a trajectory which at a high deformation $b=0.15$ escapes in only 25 iterations. If the core of the cavity is made out of a material so that the ratio of the refraction indices between the core and the outer layer is say 0.6, we see that the same trajectory is trapped inside indefinitely [Fig. 12(b)]. It can be proven by Euclidean geometry that if the index of the outer layer is smaller than the index of the inner layer, then the ray will be reinjected at a lower angle of incidence which is less likely to be in the chaotic region. To see this let us look at Fig. 13. A single light ray is shown: *ACDB*, which starts at *A*, gets refracted through the inner layer and hits the boundary again at *B*. The angle of incidence before being refracted is α_a and after refraction through the inner layer is α_b. What we need to show is that $\alpha_a > \alpha_b$, so the incidence angle decreases by this procedure. This is the same as proving that $\beta_a < \beta_b$, since $\alpha_a + \beta_a = \alpha_b + \beta_b = \Pi/2$. From the triangle *VAC* we get that

$$\angle(CAB) = \Pi - (\delta_c + \omega_c) + \angle(AVC). \tag{6}$$

From the triangle *VBD* we get that

$$\angle(DBV) = \Pi - (\delta_d + \omega_d) - \angle(DVB). \tag{7}$$

The two equalities above can be rewritten as follows:

$$\delta_c + \omega_c + \angle(CAB) = \Pi + \angle(AVC), \tag{8}$$

$$\delta_d + \omega_d + \angle(DBV) = \Pi - \angle(DVB). \tag{9}$$

Comparing the above equalities, we see that since $\Pi - \angle(DVB) < \Pi + \angle(AVC)$ and $\delta_c = \delta_d$, we must have $\angle(CAB) > \angle(DBV)$ which can be written as follows: $\beta_a + \angle(OBA) > \beta_b + \angle(OAB)$. The angles $\angle(OAB)$ and $\angle(OBA)$ being equal, we get that $\beta_a > \beta_b$.

This is a very effective way of prolonging trajectories since any trajectory which hits the inner layer will be trapped inside indefinitely. Only trajectories that do not hit the inner layer soon enough will escape. These are trajectories that are really close to the escape limit initially. By reducing the size of the inner layer, more trajectories are likely to escape whereas the ones trapped inside will stay there indefinitely. The idea of designing the cavity out of layers of different refraction index can be used to make trajectories escape faster, by taking the index of the outer layer larger then that of the inner layer a trajectory. One can prove by Euclidean geometry that by doing so a trajectory will get reinjected at a higher angle of incidence, where chaos is present according to the structure of the phase space.

IV. CONCLUSIONS

We have addressed the problem of controlling the residence time of light inside dielectric microcavities, where escape occurs when the cavity undergoes deformations from

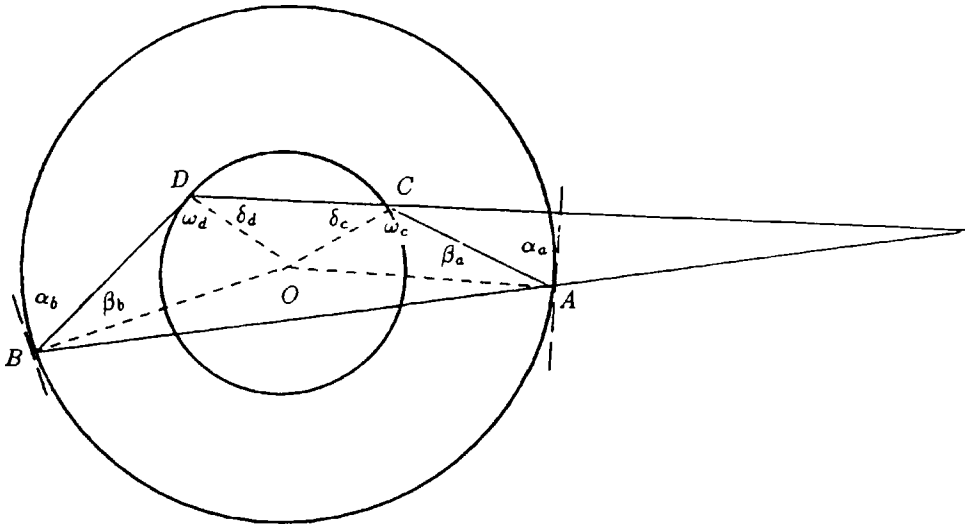

FIG. 13. A single light ray crossing a two-layer microdisk. The incidence angles are α_a and α_b.

the spherical or cylindrical shape. As explained by a ray-optics model, the escape is linked to the presence of chaos as the deformation increases. We have presented open loop control procedures for shortening or prolonging the mean escape time of light inside the cavity. One approach was to apply extra deformations to the cavity periodically, and we have shown that small regular deformations will lead to dumping out stored light with predictable escape time. This method has the potential for being applied in real situations at low deformation, where control could be implemented electro-optically [11]. Few pulses in the deformations parameter but large in amplitude can be used to extend the mean residence time. An alternative but efficient way to keep light inside is to design the cavity out of layers with different refraction indices of refraction [11].

Finally, we remark that, in general, closed loop control [22] and open loop control used in dynamics stabilize periodic orbits known *a priori*. However, in our case of open loop control, we are attempting to bound the regions of phase space by using geometric deformations of the boundary of the disk. The control perturbations in effect change the structure of the phase space by increasing the size and number of island chains. Such an increase forces the chaotic dynamics to ''slow'' its growth towards escape. This subject will be pursued in a future paper.

ACKNOWLEDGMENTS

The authors gratefully acknowledge Dr. Brent E. Little for useful discussions that led to this work. We also acknowledge the support of the Office of Naval Research for conducting this research. The numerical computations were done under the DOD High Performance Computing Project ''Dynamical Modeling and Control in Large Scale Coupled Structural and Electronic Systems.''

[1] Yoshihisa Yamamoto and Richart E. Slusher, Phys. Today **46**(6), 66 (1993).
[2] A. Mekis, J. U. Nockel, G. Chen, A. D. Stone, and R. K. Chang, Phys. Rev. Lett. **75**, 2682 (1995).
[3] R. E. Slusher, A. F. J. Levi, S. L. McCall, J. L. Glass, S. J. Pearton, and R. A. Logan (unpublished).
[4] R. J. Hawkins, N. K. Madsen, J. S. Kallman, M. D. Feit, C. C. Shang, B. W. Shore, and J. F. DeFord (unpublished).
[5] J. F. Owen, P. W. Barber, P. B. Dorain, and R. K. Chang, Phys. Rev. Lett. **47**, 1075 (1981).
[6] S. C. Hill and R. E. Benner, in *Optical Effects Associated with Small Particles*, edited by P. W. Barber and R. K. Chang (World Scientific, Singapore, 1988), p. 3.
[7] L. Collot, V. Lfe-Seguin, M. Brune, J. M. Raimond, and S. Haroche, Europhys. Lett. **23**, 327 (1993).
[8] L. Collot, V. Lefevre-Seguin, and S. Haroche, Europhys. Lett. **23**, 327 (1993)
[9] S. L. Mc Call, A. F. J. Levi, R. E. Shusher, S. J. Pearton, and R. A. Logan, Appl. Phys. Lett. **60**, 289 (1992).
[10] J. U. Nockel, A. D. Stone, and R. K. Chang, Opt. Lett. **19**, 1693 (1994).
[11] B. E. Little (private communication).
[12] Jens U. Nockel and A. Douglas Stone, Lett. Nature **385**, 45 (1997).
[13] Jens U. Nockel, A. Douglas Stone, Gang Chen, Helene L. Grossman, and Richard K. Chang, Opt. Lett. **21**, 1609 (1996).
[14] Edward Ott, *Chaos in Dynamical Systems* (Cambridge University Press, Cambridge, 1993).
[15] M. V. Berry, Eur. J. Phys. **2**, 91 (1981).
[16] Marko Robnik, J. Phys. A **17**, 1049 (1984); and **16**, 3971 (1983).
[17] J. U. Nockel and A. D. Stone, in *Optical Processes in Microcavities*, edited by R. K. des Chang and A. J. Campillo (World Scientific, Singapore, 1996), pp. 389–462.
[18] David S. Citrin, Steven Tomsovic, and William E. Torruellas, in *Beam Control and Switching in Nonlinear Meso-Optical Structures*, OSA Technical Digest Series Vol. 5 (Optical Society of America, Victoria, British Columbia, Canada, 1998).
[19] Ying-Cheng Lai, Mingxhon Ding, and Celso Grebogi, Phys. Rev. E **47**, 86 (1993).
[20] Zonghua Liu and Shigang Chen, Int. J. Bifurcation Chaos Appl. Sci. Eng. **8**, 1355 (1998).
[21] L. E. Reichl, *The Transition to Chaos* (Springer-Verlag, Berlin, 1992).
[22] Ira B. Schwarts, Thomas W. Carr, and Ioana Triandaf, Chaos **7**, 664 (1997).